Preparation and Properties of Molybdenum–Pentadienyl Complexes: A Facile $\eta^5 \rightleftharpoons \eta^3$ Reversible Interconversion for a Pentadienyl Ligand

Gene-Hsian Lee and Shie-Ming Peng

Department of Chemistry, National Taiwan University, Taipei, Taiwan 10764, Republic of China

Inn-Chu Tsung, David Mu, and Rai-Shung Liu*

Department of Chemistry, National Tsing Hua University, Hsinchu, Taiwan 30043, Republic of China

Received November 25, 1988

$(\eta^3\text{-}C_5H_7)Mo(\overset{\frown}{P\,P})(CO)_2Br$ ($\overset{\frown}{P\,P}$ = dppe, dmpe) reacts with $AgBF_4$ in CH_2Cl_2 to give the cations $[(\eta^5\text{-}C_5H_7)Mo(\overset{\frown}{P\,P})(CO)_2]BF_4$ ($\overset{\frown}{P\,P}$ = dppe (1), dmpe (2)). In CH_3CN, 1 and 2 each undergo rearrangement to produce the cations $[(\eta^3\text{-}C_5H_7)Mo(\overset{\frown}{P\,P})(CO)_2(CH_3CN)]BF_4$ ($\overset{\frown}{P\,P}$ = dppe (3), dmpe (4)). Compounds 3 and 4 can be alternatively prepared by the reaction between $AgBF_4$ and $(\eta^3\text{-}C_5H_7)Mo(\overset{\frown}{P\,P})(CO)_2Br$ in CH_3CN. In $CHCl_3$ and CH_3COCH_3, the η^3 cations 3 and 4 readily lose CH_3CN to re-form 1 and 2 and reach equilibrium. The $\eta^3 \rightleftarrows \eta^5$ equilibrium constants in $CDCl_3$ and CD_3COCD_3 were determined from ^{31}P NMR spectra. The molecular structure of 1 has been determined from an X-ray diffraction study. Crystallographic data: space group $P\bar{1}$, a = 10.739 (2) Å, b = 11.292 (3) Å, c = 14.428 (3) Å, α = 93.53°, β = 79.42 (2)°, γ = 116.60 (3)°, Z = 2, R_F = 0.035, and R_w = 0.028.

Introduction

In recent years, there has been a resurgence of interest in the chemistry of acyclic transition-metal–pentadienyl complexes.[1] Numerous studies[1-4] have focused on a comparison of the structural and reaction chemistry of the η^5-pentadienyl complexes with that of their cyclopentadienyl analogues. Theoretical studies have shown that the resonance energy of a η^5-pentadienyl group is smaller than that of a η^5-cyclopentadienyl group,[5] and hence the interconversion η^5–η^3 is better operable for the metal–pentadienyl system. In the metal pentadienyl system, the observation of this process has been reported in several studies. According to an earlier paper by Powell,[6] $(\eta^5\text{-}C_5H_7)Mn(CO)_3$ reacts with phosphine ligands to produce $(\eta^3\text{-}C_5H_7)Mn(CO)_3PR_3$ which upon heating loses CO to generate $(\eta^5\text{-}C_5H_7)Mn(CO)_2(PR_3)$. Bleeke[7] has recently reported an $\eta^5 \rightleftarrows \eta^3$ interconversion mode involving $(\eta^5\text{-}C_5H_7)(\eta^3\text{-}C_5H_7)Fe(PR_3)$ and $(\eta^3\text{-}C_5H_7)_2Fe(PR_3)_2$. Ernst[8] has found that $CpCr(\eta^5\text{-}C_5H_7)(CO)$ reacts with CO to give $CpCr(\eta^3\text{-}C_5H_7)(CO)_2$ which in turn readily loses CO upon photoexcitation to give the η^5-pentadienyl compound. In this paper, we report a reversible $\eta^5 \rightleftarrows \eta^3$ rearrangement involving the complexes $[(\eta^5\text{-}C_5H_7)Mo(\overset{\frown}{P\,P})(CO)_2]^+$ and $[(\eta^3\text{-}C_5H_7)Mo(\overset{\frown}{P\,P})(CO_2)(CH_3CN)]^+$ ($\overset{\frown}{P\,P}$ = dppe, dmpe).

Scheme I

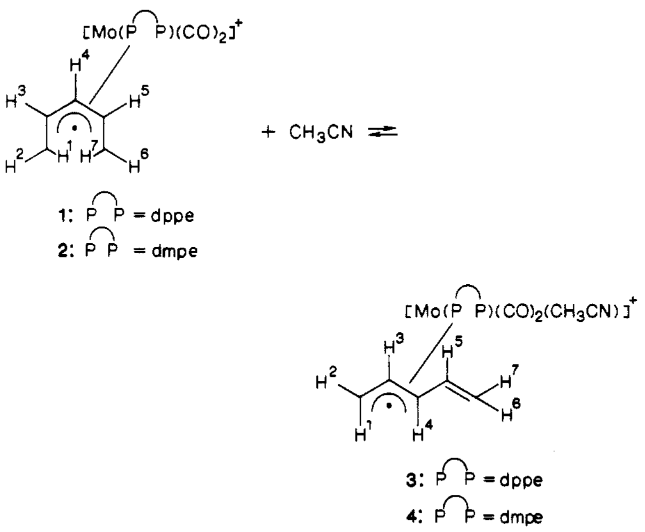

One interesting feature of this interconversion is that the system is observed to be in a state of equilibrium between the two forms.

Results and Discussion

Synthesis. Stirring of $(\eta^3\text{-}C_5H_7)Mo(CO)_2(\overset{\frown}{P\,P})Cl$[9] ($\overset{\frown}{P\,P}$ = dppe, dmpe) with an equimolar amount of $AgBF_4$ in CH_2Cl_2 gave the cations $[(\eta^5\text{-}C_5H_7)Mo(CO)_2(\overset{\frown}{P\,P})]BF_4$ ($\overset{\frown}{P\,P}$ = dppe (1), dmpe (2)) in good yields after workup. Recrystallization from CH_2Cl_2/ether produced yellow crystals of 1 and orange crystals of 2. Compounds 1 and 2 have an asymmetric U-shaped pentadienyl group as indicated by the very upfield chemical shifts of the two anti protons H^1 and H^7 within δ −0.10 to 1.00 ppm. An X-ray diffraction study of 1 was performed to elucidate the molecular structure. An ORTEP drawing of the molecular structure is shown in Figure 1. Atomic coordinates for

---

[1] For recent reviews of transition-metal acyclic pentadienyl complexes, see: (a) Ernst, R. D. *Acc. Chem. Res.* **1985**, *15*, 56. (b) Yasuda, H.; Nakamura, A. *J. Organomet. Chem.* **1985**, *285*, 15. (c) Powell, P. *Adv. Organomet. Chem.* **1986**, *26*, 125.

[2] (a) Bleeke, J. R.; Rauscher, D. J.; Moore, D. A. *Organometallics* **1987**, *6*, 2614. (b) Bleeke, J. R.; Peng, W.-J. *Ibid.* **1986**, *5*, 635.

[3] (a) Kralik, M. S.; Hutchinson, J. P.; Ernst, R. D. *J. Am. Chem. Soc.* **1985**, *107*, 8296. (b) Kralik, M. S.; Rheingold, A. L.; Ernst, R. D. *Organometallics* **1987**, *6*, 2612.

[4] Bleeke, J. R.; Kotyk, J. J. *Organometallics* **1985**, *4*, 194.

[5] Bohm, M. C.; Eckert-Maksic, M.; Ernst, R. D.; Wilson, D. R.; Gleiter, R. *J. Am. Chem. Soc.* **1984**, *106*, 1646. (b) Gleiter, R.; Bohm, M. C.; Ernst, R. D. *J. Electron Spectrosc. Phenom. Relat.* **1984**, *33*, 269.

[6] Paz-Sandoval, M. A.; Powell, P.; Drew, M. G. B.; Perutz, R. N. *Organometallics* **1984**, *3*, 1026.

[7] Bleeke, J. R.; Hays, M. K.; Wittenbrink, R. J. *Organometallics* **1988**, *7*, 1417.

[8] Freeman, J. W.; Ernst, R. D. Presented at the 196th American Chemical Society National Meeting, Los Angeles, Sept 1988.

[9] Lee, G.-H.; Peng, S.-M.; Liu, F.-C.; Mu, D.; Liu, R.-S. *Organometallics* **1989**, *8*, 402.

0276-7333/89/2308-2248$01.50/0

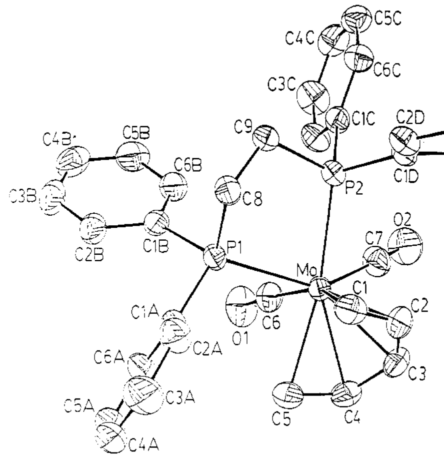

Figure 1. Molecular structure of the (η^5-C_5H_7)Mo(CO)$_2$(dppe) cation (1).

Table I. Bond Distances (Å) and Angles (deg) of Molecular 1

Mo–P(1)	2.5361 (10)	P(2)–C(1C)	1.825 (3)
Mo–P(2)	2.5009 (13)	P(2)–C(1D)	1.834 (3)
Mo–C(1)	2.396 (3)	C(1)–C(2)	1.368 (6)
Mo–C(2)	2.345 (3)	C(2)–C(3)	1.419 (5)
Mo–C(3)	2.306 (3)	C(3)–C(4)	1.398 (5)
Mo–C(4)	2.320 (3)	C(4)–C(5)	1.370 (5)
Mo–C(5)	2.351 (3)	C(6)–O(1)	1.144 (4)
Mo–C(6)	1.971 (3)	C(7)–O(2)	1.135 (4)
Mo–C(7)	2.000 (3)	C(8)–C(9)	1.525 (4)
P(1)–C(8)	1.828 (3)	B–F(1)	1.373 (5)
P(1)–C(1A)	1.805 (3)	B–F(2)	1.347 (5)
P(1)–C(1B)	1.833 (3)	B–F(3)	1.374 (5)
P(2)–C(9)	1.850 (3)	B–F(4)	1.320 (5)

P(1)–Mo–P(2)	76.52 (4)	C(6)–Mo–C(7)	80.12 (13)
P(1)–Mo–C(1)	83.49 (10)	Mo–P(1)–C(8)	107.23 (10)
P(1)–Mo–C(2)	117.01 (10)	Mo–P(1)–C(1A)	114.03 (10)
P(1)–Mo–C(3)	138.78 (10)	Mo–P(1)–C(1B)	121.31 (11)
P(1)–Mo–C(4)	120.28 (10)	C(8)–P(1)–C(1A)	107.94 (14)
P(1)–Mo–C(5)	86.21 (9)	C(8)–P(1)–C(1B)	101.69 (13)
P(1)–Mo–C(6)	82.26 (9)	C(1A)–P(1)–C(1B)	103.43 (14)
P(1)–Mo–C(7)	141.66 (10)	Mo–P(2)–C(9)	111.88 (9)
P(2)–Mo–C(1)	86.09 (9)	Mo–P(2)–C(1C)	120.24 (10)
P(2)–Mo–C(2)	93.79 (9)	Mo–P(2)–C(1D)	113.22 (9)
P(2)–Mo–C(3)	122.12 (10)	C(9)–P(2)–C(1C)	101.50 (13)
P(2)–Mo–C(4)	157.31 (9)	C(9)–P(2)–C(1D)	105.40 (13)
P(2)–Mo–C(5)	157.20 (10)	C(1C)–P(2)–C(1D)	102.96 (13)
P(2)–Mo–C(6)	109.89 (9)	Mo–C(1)–C(2)	71.19 (20)
P(2)–Mo–C(7)	77.92 (9)	Mo–C(2)–C(1)	75.29 (19)
C(1)–Mo–C(2)	33.52 (13)	Mo–C(2)–C(3)	70.76 (19)
C(1)–Mo–C(3)	63.73 (14)	C(1)–C(2)–C(3)	126.0 (3)
C(1)–Mo–C(4)	81.30 (13)	Mo–C(3)–C(2)	73.73 (19)
C(1)–Mo–C(5)	77.14 (13)	Mo–C(3)–C(4)	72.96 (20)
C(1)–Mo–C(6)	155.32 (13)	C(2)–C(3)–C(4)	127.4 (4)
C(1)–Mo–C(7)	122.66 (13)	Mo–C(4)–C(3)	71.86 (19)
C(2)–Mo–C(3)	35.51 (14)	Mo–C(4)–C(5)	74.20 (19)
C(2)–Mo–C(4)	65.56 (13)	C(3)–C(4)–C(5)	124.8 (4)
C(2)–Mo–C(5)	80.77 (13)	Mo–C(5)–C(4)	71.69 (20)
C(2)–Mo–C(6)	152.93 (12)	Mo–C(6)–O(1)	174.8 (3)
C(2)–Mo–C(7)	92.69 (14)	Mo–C(7)–O(2)	177.1 (3)
C(3)–Mo–C(4)	35.18 (13)	P(1)–O(8)–C(9)	108.07 (19)
C(3)–Mo–C(5)	63.58 (13)	P(2)–C(9)–C(8)	112.05 (19)
C(3)–Mo–C(6)	117.51 (13)	F(1)–B–F(2)	113.3 (3)
C(3)–Mo–C(7)	79.40 (14)	F(1)–B–F(3)	106.8 (3)
C(4)–Mo–C(5)	34.11 (13)	F(1)–B–F(4)	108.7 (4)
C(4)–Mo–C(6)	88.63 (13)	F(2)–B–F(3)	109.1 (3)
C(4)–Mo–C(7)	93.10 (13)	F(2)–B–F(4)	111.5 (4)
C(5)–Mo–C(6)	81.89 (13)	F(3)–B–F(4)	107.1 (4)
C(5)–Mo–C(7)	124.21 (13)		

Table II. Final Atomic Coordinates for Molecular 1

	x	*y*	*z*	B_{iso}, Å^2
Mo	0.33598 (3)	0.206642 (25)	0.206710 (18)	2.221 (13)
P(1)	0.56248 (8)	0.28242 (7)	0.27246 (5)	2.35 (4)
P(2)	0.34102 (8)	0.39529 (7)	0.30891 (5)	2.37 (4)
C(1)	0.4849 (4)	0.3717 (4)	0.08675 (23)	3.41 (20)
C(2)	0.3502 (4)	0.3130 (4)	0.06787 (22)	3.69 (20)
C(3)	0.2647 (4)	0.1748 (4)	0.06208 (23)	3.86 (21)
C(4)	0.2990 (4)	0.0723 (4)	0.07627 (24)	3.60 (21)
C(5)	0.4260 (4)	0.0900 (4)	0.09621 (25)	3.35 (19)
C(6)	0.2782 (3)	0.0481 (3)	0.28562 (21)	3.06 (16)
C(7)	0.1300 (4)	0.1571 (3)	0.24674 (23)	3.60 (19)
C(8)	0.6290 (3)	0.4604 (3)	0.29163 (20)	2.64 (15)
C(9)	0.5105 (3)	0.4839 (3)	0.35261 (20)	2.66 (15)
C(1A)	0.6997 (3)	0.2559 (3)	0.19503 (20)	2.84 (16)
C(2A)	0.8045 (4)	0.3528 (3)	0.13267 (24)	3.95 (19)
C(3A)	0.9019 (4)	0.3223 (4)	0.0700 (3)	5.06 (22)
C(4A)	0.8951 (4)	0.1997 (5)	0.0714 (3)	5.4 (3)
C(5A)	0.7919 (5)	0.1022 (4)	0.1335 (3)	4.98 (25)
C(6A)	0.6933 (4)	0.1292 (3)	0.19446 (23)	3.79 (18)
C(1B)	0.5620 (3)	0.2215 (3)	0.38744 (21)	2.78 (16)
C(2B)	0.6819 (3)	0.2161 (3)	0.40778 (23)	3.58 (18)
C(3B)	0.6822 (4)	0.1826 (3)	0.4986 (3)	4.52 (22)
C(4B)	0.5679 (5)	0.1563 (3)	0.56935 (25)	4.67 (24)
C(5B)	0.4502 (4)	0.1617 (3)	0.54985 (24)	4.29 (22)
C(6B)	0.4478 (4)	0.1931 (3)	0.45925 (22)	3.47 (18)
C(1C)	0.2131 (3)	0.3648 (3)	0.41796 (19)	2.63 (15)
C(2C)	0.1419 (3)	0.2397 (3)	0.46109 (22)	3.37 (17)
C(3C)	0.0574 (4)	0.2198 (3)	0.54811 (24)	4.31 (19)
C(4C)	0.0373 (4)	0.3217 (4)	0.59250 (22)	4.13 (19)
C(5C)	0.1038 (4)	0.4455 (3)	0.55033 (23)	3.86 (19)
C(6C)	0.1924 (3)	0.4682 (3)	0.46361 (21)	3.41 (17)
C(1D)	0.3217 (3)	0.518 (3)	0.24738 (19)	2.57 (15)
C(2D)	0.4384 (3)	0.6374 (3)	0.20995 (21)	3.15 (16)
C(3D)	0.4190 (4)	0.7281 (3)	0.16116 (23)	4.13 (21)
C(4D)	0.2869 (4)	0.7055 (3)	0.14921 (25)	4.38 (22)
C(5D)	0.1719 (4)	0.5913 (4)	0.18571 (24)	4.27 (21)
C(6D)	0.1882 (3)	0.4987 (3)	0.23474 (22)	3.36 (18)
O(1)	0.2477 (3)	−0.04821 (22)	0.32547 (17)	4.89 (15)
O(2)	0.0133 (3)	0.1268 (3)	0.27283 (18)	5.59 (16)

atoms other than hydrogen are given in Table I, whereas selected bond distances and angles are given in Table II. The coordination geometry about the molybdenum center is closed to a distorted square pyramid with the P(1), P(2), C(6), and C(7) atoms occupying the four basal sites. One chelating phosphorus atom is situated beneath the open mouth of the dienyl ligand, whereas the other lies below the edge. An interesting feature is that the P(1), Mo, and C(7) atoms lie on a line which nearly bisects the pentadienyl plane. Such a stereochemistry fully agrees with the predicted geometry for the (η^5-C_5H_7)ML$_4$ system.[10] Bond lengths of Mo–P(1) and Mo–P(2) are 2.5361 (10) Å and 2.5009 (13) Å, respectively. The distances between the molybdenum atom and the five carbons of the pentadienyl group are 2.306 (3)–2.396 (3) Å; these bond distances are nearly equal to those (2.319 (5)–2.355 (6) Å) of the neutral Mo(II)-dienyl compound I. In 1, the C–C bond distances in the C(1)–C(5) fragment (1.368 (6), 1.419 (5), 1.398 (5), 1.370 (5) Å) are smaller than the corresponding distances of the molecule I[3b] (1.418 (7), 1.424 (6), 1.410 (7), 1.404 (6) Å). The P(1) atom is 2.205 (8) Å from the pentadienyl plane, compared with 3.302 (4) Å for the P(2) atom.

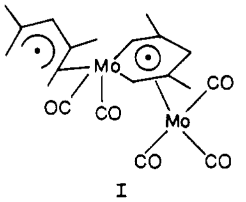

I

$\eta^5 \rightleftarrows \eta^3$ **Interconversion.** One interesting feature of these η^5 cations is the observation that the complexes readily undergo $\eta^3 \rightleftarrows \eta^5$ rearrangement in CH_3CN solution. When crystals of 1 and 2 were dissolved in CH_3CN, new

---

[10] Albright, T. A.; Hoffmann, R.; Tse, Y.-C.; D'Ottavio, T. *J. Am. Chem. Soc.* **1979**, *101*, 3812.

ν(CO) lines in the IR spectrum appeared at ~1955 (s) and ~1865 (s) cm^{-1}, concurrently with the disappearance of ν(CO) lines at ~1985 (s) and ~1915 (s) cm^{-1} assigned to the η^5 cations. The two new lines at ~1955 (s) and ~1865 (s) cm^{-1} are assigned to $[(syn\text{-}\eta^3\text{-}C_5H_7)Mo(CO)_2(P^\frown P)(CH_3CN)]BF_4$ ($P^\frown P$ = dppe (**3**), dmpe (**4**)). Isolation of **3** and **4** was achieved by removal of CH_3CN, followed by recrystallization from CH_3CN/ether, yielding yellow crystals of **3** and **4**. The compounds have been characterized by elemental analysis and IR and ^1H and ^{31}P NMR spectra. The syn configuration of the dienyl ligand is indicated by the ^1H NMR coupling constants $J_{13} = J_{34} = 10.2$ Hz and $J_{23} = 7.2$ Hz. An alternative preparation of **3** and **4** was also achieved by means of the reaction between $AgBF_4$ and $(\eta^3\text{-}C_5H_7)Mo(CO)_2(P^\frown P)Br$ in CH_3CN; the yield is 80–85%.

Compounds **3** and **4** readily lose the coordinated CH_3CN in solvents other than acetonitrile and re-form the η^5 cations **1** and **2**, respectively. When **3** was dissolved in $CDCl_3$ and CD_3COCD_3, monitored by IR and NMR spectroscopy, an equilibrium, $\mathbf{1} \rightleftarrows \mathbf{3}$, was reached in 10 h. Compound **4**, however, underwent a complete conversion to **2** when the solution (in CD_3COCD_3 or $CDCl_3$) was allowed to stand for 10 h. Readdition of a small proportion of CD_3CN to this solution led to the reappearance of the ^1H NMR signals of **4**. As the interconversion was found to be in a state of dynamic equilibrium, NMR spectra were used for calculation of the equilibrium constants K (mol/L) defined by the equation $K = [\eta^5][CH_3CN]/[\eta^3\text{-}CH_3CN]$. The constants were more precisely measured from the ^{31}P NMR spectra because all the complexes show a well-defined AB pattern in the resonances of the two nonequivalent phosphorus atoms. The K values for $\mathbf{2} \rightleftarrows \mathbf{4}$ were 1.28 ± 0.10 M and 3.58 ± 0.10 M in $CDCl_3$ and CD_3COCD_3, respectively; for $\mathbf{1} \rightleftarrows \mathbf{3}$, the K values were $(7.0 \pm 0.3) \times 10^{-2}$ M and $(8.2 \pm 0.3) \times 10^{-2}$ M in $CDCl_3$ and CD_3COCD_3, respectively. These values indicate that the bidentate ligand dmpe tends to stabilize the η^5-structure more effectively than the dppe ligand. The enhancement of the metal electron density by the dmpe ligand appears to strengthen metal–ligand bonding through donation of metal d electrons to the empty ligand orbital. We do not preclude the possibility that the more congested structure of **1** tends to favor the η^3 geometry.

The $\eta^5 \leftrightarrow \eta^3$ interconversion has been known for metal–cyclopentadienyl[11] and -pentadienyl complexes.[6-8] This reaction mode generally involves soft ligands such as nitric oxide, carbon monoxide, and phosphines. In the η^5 cations **1** and **2**, a labile ligand like CH_3CN surprisingly causes $\eta^5 \rightarrow \eta^3$ slippage; more interestingly the interconversion is observed to be in a state of dynamic equilibrium. This observation reflects that the η^5–η^3 interconversion is better operable for metal–pentadienyl compounds than for their cyclopentadienyl analogues.

Dynamic NMR Studies. The NMR spectra of **1** and **2** at ambient temperatures are consistent with the asymmetric orientation of the bis(phosphine) ligand observed in the solid-state structure. The two ends of the chelating phosphines and the two ends of the pentadienyl ligand are inequivalent. The $^{31}P\{H\}$ NMR spectra show a distinct AB quartet pattern, and the ^1H NMR spectra exhibit seven distinct signals for the pentadienyl protons. However, with increase of temperature, the rate of the pentadienyl rotation with respect to the bis(phosphine) fragment increases. The AB pattern in ^{31}P NMR spectra begins to broaden and to coalesce. Similar behavior is observed in the temperature-dependent ^1H NMR spectra of the pentadienyl hydrogens. This process shows the creation of a mirror plane bisecting the pentadienyl plane and in turn exchanges the ends of the bis(phosphine) ligand. The calculation of $\Delta G^{\ddagger}$ based on variable-temperature ^{31}P NMR spectra leads to a value 18.2 ± 0.2 kcal mol^{-1} (in 1,2-$C_2D_4Cl_2$) for **1** and 14.7 ± 0.2 kcal mol^{-1} (in 1,2-$C_2D_4Cl_2$) for **2**.

Scheme II. A Proposed Exchanging Mechanism Involving the Metal-η^5-Dienyl Bond Rotation

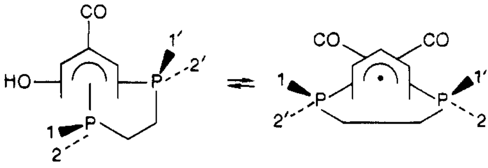

Scheme III. A Proposed Exchanging Mechanism Involving an η^3-Allyl Intermediate

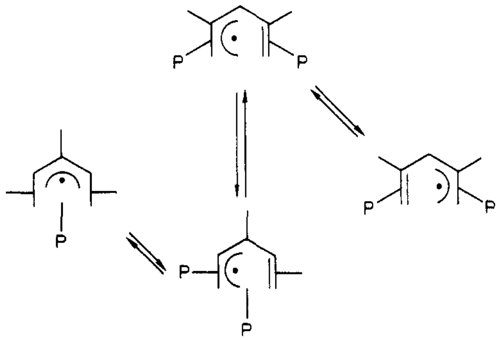

Scheme IV. Basic Skeletal Rearrangement in a Pseudorotation-Like Mechanism^a

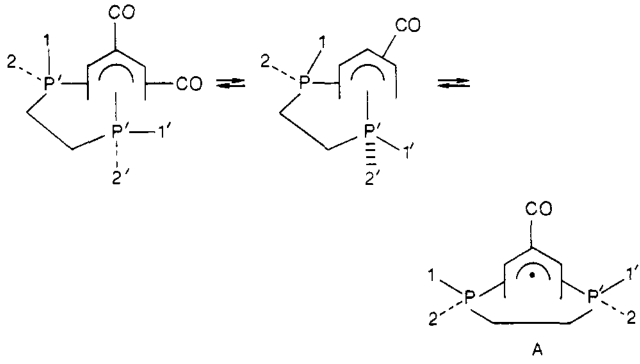

^{a} Intermediate A represents a trigonal-bipyramidal structure which allows the site exchanges to be operative $P \rightleftarrows P'$, $1 \rightleftarrows 1'$, $2 \rightleftarrows 2'$.

Three plausible mechanisms may be based on our dynamic NMR data: (1) a simple metal–dienyl bond rotation in the η^5 mode (Scheme II); (2) (a) η^5–η^3 rearrangement and then (b) rotation of the metal–η^3-allyl bond, followed by (c) rearrangement to η^5 form (Scheme III); (3) a pseudorotation-like mechanism (polytopal rearrangement) involving a square-pyramid–trigonal-bipyramid interconversion (Scheme IV). Mechanism I is a more common process for most asymmetric U-shaped pentadienyl complexes: mechanism II has been observed for $(\eta^5\text{-}C_5H_7)Re(PR_3)_3$ and $(\eta^5\text{-}C_5H_7)Mn(PR_3)_3$.[12] The pseudorotation-like mechanism has been established for $C_5H_5MoL_4$ complexes.[13] All three processes would lead to averaging of the

---

[11] (a) Bottomly, F.; Darkwa, J.; White, J. S. *J. Chem. Soc., Chem. Commun.* **1982**, 1039. (b) Casey, C. P.; O'Connor, J. M.; Haller, J. K. *J. Am. Chem. Soc.* **1985**, *107*, 1241. (c) Casey, C. P.; O'Connor, J. M.; Jones, W. D. *Organometallics* **1983**, *2*, 535.

[12] (a) Bleeke, J. R.; Moore, D. A. *Inorg. Chem.* **1986**, *25*, 3522. (b) Bleeke, J. R.; Donaldson, A. J. *Organometallics* **1986**, *5*, 2401.

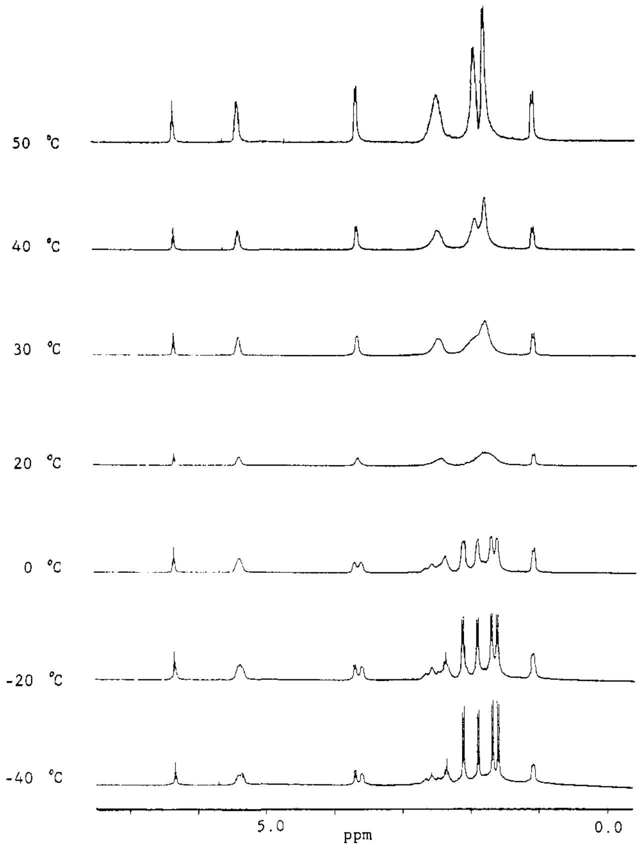

Figure 2. Variable-temperature ^{1}H NMR spectra of (η^5-C_5H_7)Mo(CO)$_2$(dmpe) (2) in 1,2-$C_2D_4Cl_2$.

phosphorus atoms and the two ends of the pentadienyl protons.

In complexes 1 and 2, external ligands readily promote the complexes to the η^3 geometries. In this manner, the energy states of the 16-e η^3 intermediates should be decreased significantly, and the $\Delta G^\ddagger$ values of the process are expected to be smaller in polar solvents than in nonpolar solvents. The measurement of $\Delta G^\ddagger$ of 2 in CD_3COCD_3 and DMF-d_7 gave 14.4 ± 0.2 and 14.6 ± 0.2 kcal mol^{-1}, respectively. These values are nearly equal to that (14.7 ± 0.2 kcal mol^{-1}) for $CDCl_3$. Therefore, mechanism II appears not to be an appropriate process as the $\Delta G^\ddagger$ values of the fluxional process were not affected by solvent polarity. In order to examine further the factors in the exchange process, we studied the rearrangement behavior of the four methyl groups. Figure 2 shows the temperature-dependent ^{1}H NMR resonances in 1,2-$C_2D_4Cl_2$ including the four methyl groups in the δ 1.60–2.20 ppm region. Notably, these four distinct methyl groups are averaged to two methyl groups with coalescing temperatures nearly identical with those of the two phosphorus nuclei. No further site exchanges between the two methyl groups were observed at elevated temperatures (60–90 °C). These NMR observations, however, were in accord with both metal–η^5-dienyl rotation and pseudorotation-like mechanisms. As depicted in Scheme I, the average form of the metal–η^5-dienyl rotation mechanism is expected to show two methyl groups ((1 $\rightleftarrows$ 1′, 2 $\rightleftarrows$ 2′). A similar behavior is also expected in the pseudorotation-like mechanism, in which the site exchanges 1 $\rightleftarrows$ 1′ and 2 $\rightleftarrows$ 2′ are operative. Therefore, at the present state, we have insufficient data to differentiate between these two mechanisms.

Conclusion

Complexes 1–4 were prepared from (η^3-C_5H_7)Mo(CO)$_2$(P$\frown$P)Br and $AgBF_4$ in CH_2Cl_2 or CH_3CN. An X-ray diffraction study of 1 reveals a square-pyramidal structure in accord with an early theoretical prediction. In solution, the two bidentate phosphorus atoms of 1 and 2 undergo mutual exchange at elevated temperatures. The pseudorotation-like mechanism and simple metal–dienyl rotation are likely to be the exchange mechanism based on the measured values of $\Delta G^\ddagger$ in various solvents. An interesting feature of these cations is their facile $\eta^5 \rightleftarrows \eta^3$ pentadienyl rearrangement. The process was observed to be in an equilibrium state. These results truly reflect a feasible $\eta^5 \rightleftarrows \eta^3$ interconversion mode for a pentadienyl ligand. This rearrangement readily provides a coordination unsaturation site and possibly gives rise to novel chemistry. Current studies in this direction are in progress.

Experimental Section

A. General Procedures. All manipulations were carried out under argon atmosphere or by Schlenk techniques. Tetrahydrofuran and ether were dried over sodium/benzophenone and distilled before use. CH_2Cl_2 and $CHCl_3$ were dried over P_2O_5 and distilled. CH_3CN was dried over CaH_2. Bis(dimethylphosphine)ethane (dmpe), bis(diphenylphosphine)ethane (dppe), and molybdenum carbonyl were obtained from Strem Chemicals and used without purification. The synthesis and spectroscopic data of Mo(η^3-C_5H_7)(CO)$_2$(P$\frown$P)X (P$\frown$P = dmpe, dppe) have been described in our previous paper.[9]

NMR spectra were measured on a Bruker AM-400 (^{1}H 400.1 MHz) or a JEOL FX-100 (^{31}P 40.25 MHz) spectrophotometer, by reference to tetramethylsilane and H_3PO_4, respectively. Microanalyses were performed by the microanalytical laboratory at National Taiwan University, Taipei, Taiwan.

B. Synthesis of [(η^5-C_5H_7)Mo(CO)$_2$(dppe)]BF_4 (1). (η^3-C_5H_7)Mo(CO)$_2$(dppe)Br (0.50 g, 0.71 mmol) was dissolved in 20 mL of CH_2Cl_2, and 0.14 g of $AgBF_4$ (0.717 mmol) was added. The resulting yellow solution was filtered and passed through a 5-cm silica column. Following removal of CH_2Cl_2, the resulting solid was crystallized from CH_2Cl_2/ether to give yellow block crystals of 1 (0.36 g, 72%). Anal. Calcd for $C_{33}H_{31}MoO_2BF_4P_2$: C, 56.27; H, 4.43. Found: C, 56.54; H, 4.88. IR spectrum (CH_2Cl_2): ν(CO) 1980 (s), 1930 (s) cm^{-1}. ^{1}H NMR (400 MHz, $CDCl_3$): δ −0.05 (1 H, m, H^1), 0.30 (1 H, m, H^7), 2.60–2.74 (2 H, m, P–CH_2), 2.80–2.90 (2 H, m, PCH_2), 3.50 (1 H, m, H^2), 3.70 (1 H, m, H^6), 3.80 (1 H, m, H^5), 5.00 (1 H, m, H^3), 6.10 (1 H, t, H^4), 7.30–7.70 (20 H, m, C_6H_5), $J_{34} = J_{45} = 3.2$ Hz, $J_{23} = J_{56} = 7.8$ Hz, $J_{13} = 11.4$ Hz. ^{31}P NMR (40.25 MHz, $CDCl_3$): δ 65.2 (d), 59.7 (d), $J_{PP'} = 36.8$ Hz.

C. Synthesis of [(η^5-C_5H_7)Mo(CO)$_2$(dmpe)]BF_4 (2). This complex was obtained similarly from the reaction between (η^3-C_5H_7)Mo(CO)$_2$(dmpe)Br (0.5 g, 1.11 mmol) and $AgBF_4$ (0.217 g, 1.11 mol) in 20 mL of CH_2Cl_2. Yellow crystals of 2 (0.44 g, 0.98 mmol, 88%) were obtained after recrystallization from CH_2Cl_2/ether. Anal. Calcd for $C_{13}H_{23}MoO_2P_2BF_4$ (2): C, 34.23; H, 5.08. Found: C, 34.52; H, 5.18. IR spectrum (CH_2Cl_2): ν(CO) 1983 (s), 1916 (s) cm^{-1}. ^{1}H NMR (400 MHz, CD_3COCD_3): δ 0.94–1.02 (2 H, complex m, H^1 + H^7), 1.62 (3 H, d, P–CH_3), 1.70 (3 H, d, P–CH), 1.90 (3 H, d, P–CH_3), 2.08 (3 H, d, P–CH_3), 3.47–3.58 (2 H, complex m, H^2 + H^6), 5.18–5.30 (2 H, complex m, H^3 + H^5), 6.62 (1 H, t, H^4), $J_{34} = J_{45} = 4.2$ Hz, $J_{23} = 2.8$ Hz, $J_{13} = 13.1$ Hz. ^{31}P NMR (40.25 MHz, $CDCl_3$): δ 37.2 (d), 40.9 (d); $J_{PP'} = 35.4$ Hz.

D. Synthesis of [(η^3-C_5H_7)Mo(CO)$_2$(dppe)(CH_3CN)]BF_4 (3). Method A. (η^3-C_5H_7)Mo(CO)$_2$(dppe)Br (0.50 g, 0.71 mmol) was dissolved in 20 mL of CH_3CN, and 0.14 g of $AgBF_4$ (0.717 mmol) was added. The resulting yellow solution was filtered and passed through 5-cm silica column. Following removal of CH_3CN, the resulting yellow solid was crystallized from CH_3CN/ether to give 0.35 g of yellow crystalline 3 (0.50 mmol, 71%). Anal. Calcd for $C_{35}H_{34}MoO_2BF_4P_2N$ (3): C, 56.43; H, 4.60. Found: C, 56.32; H, 4.84. IR spectrum (CH_3CN): ν(CO) 1956 (s), 1873 (s) cm^{-1}, ν(C=C) 1621 (w) cm^{-1}. ^{1}H NMR (400 MHz, CD_3CN): δ 2.02 (3 H, s, CH_3CN), 2.24 (1 H, d, H^1), 2.65–2.74 (2 H, m, P–CH_2), 2.88–2.98 (2 H, m, P–CH'_2), 3.52 (1 H, t, H^4), 4.15 (1 H, d, H^2),

---

(13) Faller, J. W.; Anderson, A. S. *J. Am. Chem. Soc.* **1970**, *92*, 5852.

Table III. Crystal and Diffraction Data of Molecular 1

compd	$MoP_2C_{33}H_{31}O_2BF_4$
space group	$P\bar{1}$
a, Å	10.739 (2)
b, Å	11.292 (5)
c, Å	14.428 (3)
α, deg	93.53 (3)
β, deg	79.42 (2)
γ, deg	116.60 (3)
V, Å^3	1537.40
cryst size, mm	0.15 × 0.60 × 0.65
cryst color	yellow
wavelength λ(Mo Kα), Å	0.7093
abs coeff, cm^{-1}	5.7
abs correctn	Ψ rotation
scan parameter	$0.80 + 0.35 \tan\theta$
scan type	$\omega/2\theta$
2θ range, deg	2.5–50
no. of unique reflctn	5399
no. of reflctn with $I > 3\sigma(I)$	4794
no. of variables	417
final R_F	3.0%
final R_w	2.8%[a]
final D_{map}(max), e Å^{-3}	0.67
goodness of s[b]	3.822

[a] $w = 1/(\sigma^2(F_o))$. [b] $s = [\sum w|F_o - F_c|^2/(N_o - N_c)]^{1/2}$, where N_o is the number of observations and N_c is the number of variables.

4.84 (1 H, ddd, H^3), 5.31 (1 H, d, H^7), 5.57 (1 H, d, H^6), 6.31 (1 H, dt, H^5), 7.30–7.70 (20 H, m, C_6H_5), J_{13} = 11.7 Hz, J_{23} = 7.1 Hz, J_{34} = J_{45} = 10.6 Hz, J_{56} = 16.8 Hz, J_{57} = 10.4 Hz. ^{31}P NMR (40.25 MHz, CD_3CN): δ 56.9 (d), 59.8 (d), $J_{PP'}$ = 21 Hz.

Method B. (η^3-C_5H_7)Mo(CO)$_2$(dppe)Br (0.5 g, 0.717 mmol) was dissolved in 20 mL of CH_3CN and the solution stirred for 1 h. The solution was evaporated to dryness, and the residues were crystallized from CH_3CN/ether to give 0.46 g of yellow crystals of **3** (0.65 mmol, 63%).

E. Synthesis of [(η^3-C_5H_7)Mo(CO)$_2$(dmpe)(CH_3CN)]BF_4 (4). Method A. (η^3-C_5H_7)Mo(CO)$_2$(dmpe)Br (0.50 g, 1.11 mmol) was dissolved in 20 mL of CH_3CN, and 0.22 g of $AgBF_4$ (1.11 mmol) was added. The resulting yellow solution was filtered and passed through a 5-cm silica column. After removal of CH_3CN, the resulting yellow solid was crystallized from CH_3CN/ether to give 0.42 g of yellow crystals of **4** (0.85 mmol, 76%). Anal. Calcd for $C_{15}H_{26}MoNO_2P_2BF_4$: C, 36.42; H, 4.60. Found: C, 36.42; H, 4.84. IR spectrum (CH_3CN): ν(CO) 1954 (s), 1859 (s) cm^{-1}, ν(C=C) 1617 cm^{-1}. ^{1}H NMR (400 MHz, CD_3CN): δ 1.65 (3 H, d, P-CH_3), 1.69 (3 H, d, PCH_3), 1.74 (3 H, d, PCH_3), 1.76 (3 H, d, PCH_3), 2.03 (3 H, s, CH_3CN), 2.13–2.22 (4 H, m, P-CH_2-CH_2), 2.32 (1 H, d, H^1), 3.69 (1 H, d, H^4), 3.90 (1 H, d, H^2), 5.04 (1 H, ddd, H^3), 5.30 (1 H, d, H^7), 5.56 (1 H, d, H^6), 6.37 (1 H, dt, H^5), J_{13} = 11.5 Hz, J_{23} = 7.2 Hz, J_{34} = J_{45} = 10.6 Hz, J_{56} = 16.8 Hz, J_{57} = 10.4 Hz. ^{31}P NMR (40.25 MHz, CD_3CN): δ 44.1 (d), 45.2 (d); $J_{PP'}$ = 39 Hz.

Method B. (η^3-C_5H_7)Mo(CO)$_2$(dmpe)Br (0.5 g, 1.11 mmol) was dissolved in 20 mL of CH_3CN and stirred for 1 h. The solution was evaporated to dryness, and the residues were crystallized from CH_3CN/ether to produce yellow needles of **4** (0.34 g, 0.69 mmol, 62%).

F. X-ray Diffraction Study of 1. Single crystals used for X-ray diffraction were grown from a saturated CH_2Cl_2/ether solution cooled at −20 °C. Data were collected at room temperature on a CAD4 diffractometer, using graphite-monochromated Mo Kα radiation. All data reduction and structure refinement were performed by using the NRCC-SDP-UAX. Crystal data, details of data collection, and structural analysis are summarized in Table III.

The structure of **1** was solved by the Patterson method. All atoms other than hydrogen were refined with anisotropic thermal parameters. All hydrogen atoms were added at idealized positions and included in the structure factor calculation.

G. Dynamic NMR Studies. Samples were prepared in CD_3COCD_3, $CDCl_3$, or 1,2-$C_2D_4Cl_2$, and NMR spectra were recorded over the temperature range −60 °C to 120 °C. Probe temperatures were calibrated by using the temperature dependence of the differences in chemical shift between the ^{1}H resonances of the methyl and hydroxyl groups of methanol below ambient temperatures and between the ^{1}H resonances of the methylene and hydroxyl groups of ethylene glycol above ambient temperatures.

The rate constants k_c at the coalescence temperature were calculated according to the formula

$$k_c = \pi(\Delta\nu)/2^{1/2}$$

in which $\Delta\nu$ is the difference in frequencies between the two exchanging sites in the stopped-exchange limit.[14] These rate constants were used to determine the Gibbs energy of activation $\Delta G^\ddagger$ at the coalescence temperatures T_c from the Eyring equation

$$k_c = (k'/\hbar)T_c e^{-\Delta G^\ddagger/RT_c}$$

in which k' = Boltzmann constant, $\hbar$ = Planck constant, and R = ideal gas constant.

H. Equilibrium Constant Measurement. The positions of equilibrium **1** ⇄ **3** and **2** ⇄ **4** were determined from ^{31}P NMR spectra. Samples of **3** and **4** were weighed and dissolved in a known volume of $CDCl_3$ or CD_3COCD_3. The concentrations of the solution were ca. (1.0–2.0) × 10^{-3} M. In the cases of equilibrium between **2** and **4**, added CH_3CN was present in concentrations in the range (0.4–3.0) × 10^{-3} M. The errors are reported as the standard deviation from the mean value of six runs.

Acknowledgment. We wish to thank Professors R. D. Ernst, J. R. Bleeke, and J. W. Faller for helpful comments on this work. This work was generously supported by Chinese National Science Council.

Registry No. **1**, 121810-04-6; **2**, 121810-06-8; **3**, 121810-08-0; **4**, 121810-10-4; (η^3-C_5H_7)Mo(dppe)(CO)$_2$Br, 117652-91-2; (η^3-C_5H_7)Mo(dmpe)(CO)$_2$Br, 117652-93-4; $AgBF_4$, 14104-20-2.

Supplementary Material Available: Tables of thermal parameters, atomic coordinates, and bond distances and angles (6 pages); a listing of calculated and observed structure factors (26 pages). Ordering information is given on any current masthead page.

---

[14] (a) Vrieze, K. in *Dynamic Nuclear Magnetic Resonance Spectroscopy*; Jackman, L. M., Cotton, F. A., Eds.; Academic: New York, 1975. (b) Faller, F. W. *Adv. Organomet. Chem.* **1978**, *16*, 211.